J Neurophysiol 110: 2704–2717, 2013.
First published October 2, 2013; doi:10.1152/jn.01037.2012.

Multisensory integration in early vestibular processing in mice: the encoding of passive vs. active motion

Ioana Medrea and Kathleen E. Cullen
Aerospace Medical Research Unit, Department of Physiology, McGill University, Montreal, Quebec, Canada

Submitted 30 November 2012; accepted in final form 26 September 2013

Medrea I, Cullen KE. Multisensory integration in early vestibular processing in mice: the encoding of passive vs. active motion. *J Neurophysiol* 110: 2704–2717, 2013. First published October 2, 2013; doi:10.1152/jn.01037.2012.—The mouse has become an important model system for studying the cellular basis of learning and coding of heading by the vestibular system. Here we recorded from single neurons in the vestibular nuclei to understand how vestibular pathways encode self-motion under natural conditions, during which proprioceptive and motor-related signals as well as vestibular inputs provide feedback about an animal's movement through the world. We recorded neuronal responses in alert behaving mice focusing on a group of neurons, termed vestibular-only cells, that are known to control posture and project to higher-order centers. We found that the majority (70%, $n = 21/30$) of neurons were bimodal, in that they responded robustly to passive stimulation of proprioceptors as well as passive stimulation of the vestibular system. Additionally, the linear summation of a given neuron's vestibular and neck sensitivities predicted well its responses when both stimuli were applied simultaneously. In contrast, neuronal responses were suppressed when the same motion was actively generated, with the one striking exception that the activity of bimodal neurons similarly and robustly encoded head on body position in all conditions. Our results show that proprioceptive and motor-related signals are combined with vestibular information at the first central stage of vestibular processing in mice. We suggest that these results have important implications for understanding the multisensory integration underlying accurate postural control and the neural representation of directional heading in the head direction cell network of mice.

sensory coding; self-motion; efference copy; voluntary movement; vestibular; proprioception; head movement; head direction; corollary discharge

THE ADVENT OF GENETIC ENGINEERING has resulted in numerous mutant mouse strains with behavioral phenotypes suggestive of vestibular dysfunction, including head tilting and bobbing, locomotive circling, and ataxia. Behavioral studies have characterized vestibularly driven eye movements in such mutants to gain insight into the mechanisms underlying motor learning and compensation (e.g., Beraneck et al. 2008; Faulstich et al. 2006; Katoh et al. 2008; Schonewille et al. 2001; Stahl 2004). In addition, in vitro studies (Bagnall et al. 2007, 2008; Camp et al. 2006; Nelson et al. 2003; Sekirnjak and du Lac 2002, 2006) have characterized the intrinsic membrane dynamics of neurons at the first central stage of sensory processing [i.e., vestibular nuclei (VN) neurons] in mice. However, the gap between in vitro recordings and behavior has not been bridged, since the information encoded by VN neurons in alert mice remains poorly understood.

Address for reprint requests and other correspondence: K. E. Cullen, Dept. of Physiology, McGill Univ., 3655 Prom. Sir William Osler, Montreal, Quebec, Canada H3G 1Y6 (e-mail: kathleen.cullen@mcgill.ca).

The ability to sense vestibular information is integral to the generation of reflexes that stabilize gaze and posture as well as the perception of self-motion. As an animal moves through its environment, however, self-motion cues are also available from the muscles and joints (proprioception) and motor commands producing movement (e.g., motor efference copy). Thus to understand the neural encoding of self-motion, it is vital to establish whether and how these cues are combined with vestibular signals at the level of individual neurons. To date, however, in the only in vivo characterization of the VN undertaken in awake behaving mice (Beraneck and Cullen 2007), animals were restrained such that neural sensitivities were quantified in response to passive vestibular stimulation alone.

Accordingly, to understand the encoding of self-motion under natural conditions we recorded from single VN neurons in head-unrestrained wild-type mice during passive and active movement. We addressed three important questions. First, do murine VN neurons show robust responses to passive stimulation of proprioceptors? Second, can responses to combined proprioceptive and vestibular stimulation be predicted by the weighted linear sum of responses to the individual cues? Third, are these inputs combined differently for passive vs. active movements? Our findings show that vestibular and neck proprioceptive information is integrated by single VN neurons in alert, behaving mice. However, while linear summation of the vestibular and neck sensitivities predicts well neuronal responses in passive conditions, neuronal responses are suppressed when the same motion was actively generated, with one exception. Notably, the majority of murine VN neurons display a constant and robust sensitivity to static head orientation produced by both passive and active movements. Because these neurons likely send descending projections to spinal pathways, our results suggest that the efficacy of vestibulo-spinal reflexes is reduced during active motion. Furthermore, because work in primate and cat further suggest these neurons send ascending projections to the vestibular cerebellum (Cheron et al. 1996; Reisine and Raphan 1992) and thalamus (reviewed in Cullen 2012), our results have significant implications for understanding the contribution of vestibular pathways to spatial perception in mice. Importantly, vestibular inputs are commonly thought to be vital cue for the generation of the head direction (HD) signal coded by the HD cell circuit, yet our results show that the motion information encoded at the first central stage of vestibular processing reflects the integration of allocentric (i.e., vestibular) and egocentric (i.e., proprioceptive, motor efference copy) signals. Accordingly, we speculate that this multisensory integration

contributes to the genesis of an internal representation of directional heading in mice.

METHODS

Eighteen male C-57bl6 (30–35 g; Charles River Laboratories) adult mice were included in this study. The procedures were approved by the McGill University Animal Care Committee and were in strict compliance with the guidelines of the Canadian Council on Animal Care.

Head-post implantation and craniotomy. Surgical techniques and anesthesia protocols used were adapted from those previously described by Beraneck and Cullen (2007). Briefly, mice were anesthetized with an intraperitoneal injection of a mixture of atropine (5×10^{-4} mg/g), ketamine (10^{-1} mg/g), acepromazine maleate (2.5×10^{-2} mg/g), xylazine (10^{-1} mg/g), and sterile saline. Anesthetized mice were then secured in a stereotaxic frame. A 1-mm-diameter craniotomy was performed to allow access to the VN. A dental cement chamber (C&B Metabond) was then constructed around the craniotomy, and a custom-built head holder was cemented to the implant anterior to the chamber. Following surgery, Carbapen (0.05 mg/kg) was utilized for postoperative analgesia, and antibacterial cream (2%, Astra Pharma, Ontario, Canada) was applied to the incision site to prevent infection. Animals were kept in isolated cages and closely monitored during the first 72 h.

Recording sessions. During experiments, mice were placed in a custom-built Plexiglas tube at the center of a turntable. Their heads were fixed with a stainless steel post to align the horizontal semicircular canals with the horizontal plane (i.e., 35° nose down; Calabrese and Hullar 2006; Vidal et al. 2004). Within the tube the mouse's body was further restrained by a pair of harnesses, which held its front limbs and hindlimbs (Covariance Infusion Harness). The turntable was used to apply passive vestibular rotational stimuli. Additionally, the design of the head postrestraint system allowed the experimenter to rapidly release the mouse's head during recording to allow passive (experimenter applied) and active (mouse-generated) rotations in the yaw axis. For such rotations, the animal's body remained stationary, restrained by the harness. Finally, the setup included an additional earth-stationary head post connector, to which the head was attached, allowing the experimenter to passively rotate the mouse's body under a stationary head.

Eye movements were monitored using the video-oculography method previously described by Stahl et al. (2000). Turntable velocity was measured with an angular velocity sensor (Watson Industries). Head and body position were measured with magnetic search coils (Fuchs and Robinson 1966). Extracellular single-unit activity was recorded using insulated tungsten microelectrodes (5–10 MΩ impedance, Frederic Haer). During each experiment eye, head, body and table movements as well as unit activity were recorded on digital audio tape for later playback and off-line analysis.

Behavioral paradigms. All VN neurons described in the present report were sensitive to vestibular stimulation produced by passive horizontal head rotations, but were insensitive to eye movements. Thus these neurons corresponded to a class of neurons termed "vestibular-only" (VO) neurons that have been previously described in mice (Beraneck and Cullen 2007) and primates (reviewed in Cullen 2012). To quantify response to vestibular stimulation, head-and-body restrained mice were passively (0.5 Hz, ±40°/s) rotated in the yaw

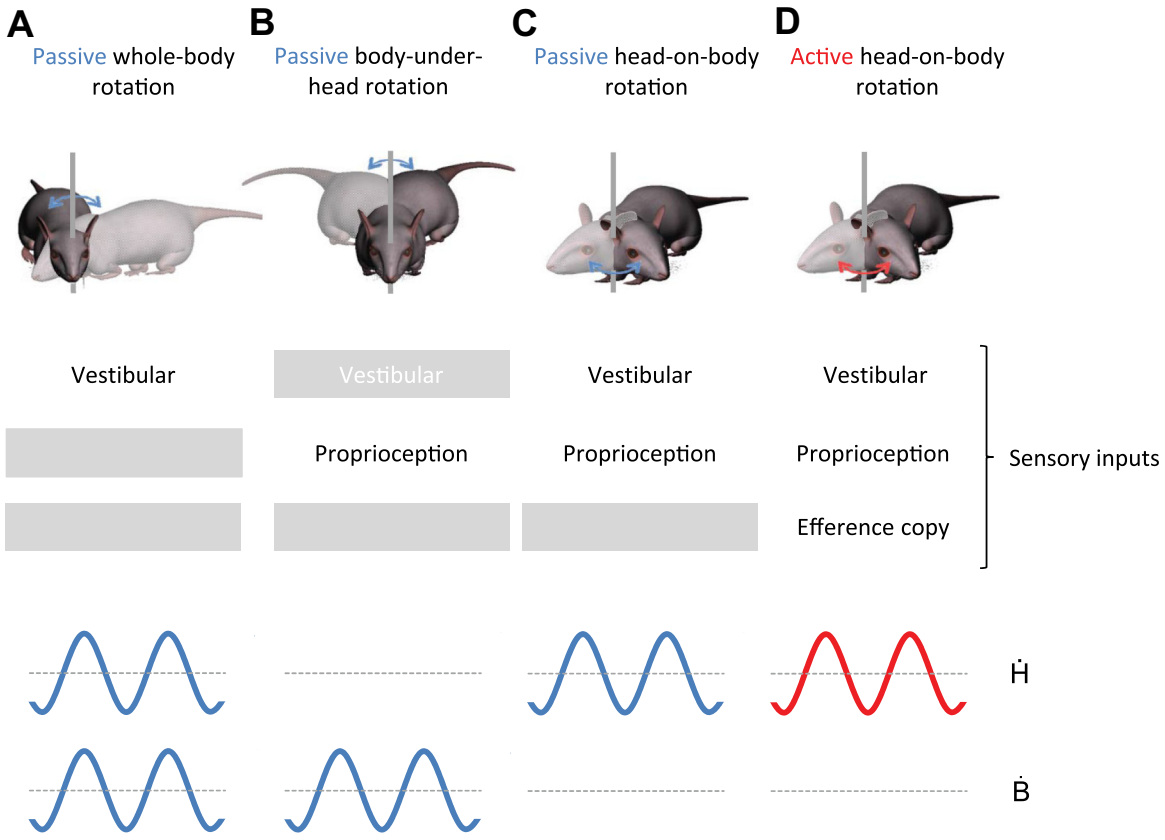

Fig. 1. Four different paradigms stimulating the vestibular and neck proprioceptive systems each separately, or in combination, were used. *A*: neuronal sensitivities to vestibular stimulation were quantified in response to horizontal head movements resulting from applied whole body rotations. *B*: neuronal sensitivities to neck proprioceptive stimulation were quantified in response to horizontal movements of the body relative to head resulting from applied body-under-head rotations. *C* and *D*: neuronal sensitivities to combined vestibular and neck proprioceptive stimulation were quantified in response to applied horizontal head-on-body rotations (*C*) and voluntarily generated horizontal head-on-body rotations (*D*). $\dot{B}$, body velocity; $\dot{H}$, head velocity.

axis using a servomotor (passive whole body rotations; Fig. 1*A*). A minimum of 20 cycles of rotation were applied for this characterization. Once vestibular-sensitive neurons were identified, we confirmed each neuron's lack of eye movement sensitivity by *1*) verifying that neurons did not burst or pause during the fast phases of the induced nystagmus; and *2*) using the static eye position protocol previously described by Beraneck and Cullen (2007). For the latter protocol, the turntable was rotated through a series of steps to drive the eye at different eccentric positions in the orbit (range of ~20°).

Having confirmed that a given neuron was sensitive to passive vestibular stimulation but insensitive to eye movements, we next characterized neuronal responses using a series of 4 different protocols designed to stimulate the vestibular and proprioceptive systems independently or in combination.

First, the mouse's head was held stationary relative to the earth while its body was sinusoidally (0.5 Hz, ±40°/s) rotated below for a minimum of 20 cycles. This paradigm, termed "body-under-head rotation" (Fig. 1*B*), was used to characterize neuronal responses to dynamic stimulation of neck proprioceptors.

Second, the mouse's head was released from the restraint and passively rotated over a range of ±20° relative to its earth stationary body. This rotation was manually preformed by the experimenter to provide a minimum of 40 movements covering the full range of possible head positions. In addition, the head was held stationary for 4 s following each rotation, and neuronal responses were measured to assess sensitivities to static changes in the orientation of the head relative to the body.

Third, the experimenter rotated the mouse's head relative to its stationary restrained body to produce head movements matching *1*) those applied during the original assessment of vestibular sensitivities (i.e., during sinusoidal passive whole body rotation); and *2*) those generated by the mouse in the active movement paradigm. Movements produced during this paradigm, termed passive "head-on-body rotation" (Fig. 1*C*) were likewise restricted to the yaw axis and resulted in the combined sensory stimulation of both the proprioceptors and vestibular horizontal semicircular canals.

Finally, neuronal responses were measured in a condition in which the mouse's head was released so that it could make active head on body rotation in the yaw axis (Fig. 1*D*). In this condition, the body of each mouse was restrained in a harness, but could make active head movements that were restricted to the yaw axis by use of a head post attached to a custom-designed holder. Thus, mice generated motor commands to move their heads, in addition to experiencing combined stimulation of both proprioceptive and vestibular sensors. To encourage mice to produce head movements, we used a variety of incentives to entice mice to orient toward edible rewards (peanut butter, granola) or away from unpleasant olfactory stimuli (permanent marker, Vick's Vaporub). Active recording sessions lasted 5 min on average, during which mice made 20 or more head movements. Note that mice were not foraging in this experimental condition, as their bodies were stationary and could only move the head on body.

Off-line analysis. During playback, data acquisition was controlled by a QNX-based real-time data-acquisition system (REX) (Hayes et al. 1982). The isolation of each unit was carefully evaluated, and action potentials were discriminated using a windowing circuit (BAK) that was set manually to generate a pulse coincident with the rising phase of each action potential. Analog signals were low-pass filtered at 250 Hz (8-pole Bessel filter) and sampled at 1,000 Hz. The data were transferred into Matlab (The MathWorks) programming environment for analysis. Eye, head, and body position signals were digitally filtered with a 51st-order finite-impulse-response filter using a cut-off frequency of 20 Hz and then digitally differentiated to obtain velocity signals. To estimate each neuron's regularity, we computed the coefficient of variation (CV) and the SD of the interspike interval/mean interspike interval in the absence of either vestibular or proprioceptive stimulation. A spike density function in which a Gaussian function was convolved with the spike train (SD of 10 ms) was utilized to represent the neuronal firing rates (Cherif et al. 2008; Cullen et al. 1996).

In our analysis of neuronal responses, we first verified that neurons were insensitive to saccadic eye movements. In addition, each neuron's lack of response to eye position was confirmed by analyzing periods of steady fixation obtained during the static eye position protocol described in Beraneck and Cullen (2007). A least-squared regression analysis was then used to quantify each unit's response to vestibular stimulation during passive whole body rotations (Fig. 1*A*):

$$\hat{fr}\left(t\right) = b + S_{v\text{-}vest}\,\dot{H}\left(t\right) + S_{a\text{-}vest}\,\ddot{H}\left(t\right) \qquad (1)$$

where $\hat{fr}$ is the estimated firing rate, $S_{v\text{-}vest}$ and $S_{a\text{-}vest}$ are coefficients representing sensitivities to head velocity and acceleration, respectively, b is a bias term, and $\dot{H}$ and $\ddot{H}$ are head velocity and head acceleration, respectively. The estimated coefficients $S_{v\text{-}vest}$ and $S_{a\text{-}vest}$ were then used to calculate each unit's sensitivity [(spikes/s)/(°/s)] and phase (°) shift relative to head velocity.

A comparable approach was next used to describe each unit's response to proprioceptive stimulation during passive sinusoidal rotation of the body under a stationary head (Fig. 1*B*) using the equation:

$$\hat{fr}\left(t\right) = b + S_{v\text{-}neck}\,\dot{B}\left(t\right) + S_{a\text{-}neck}\,\ddot{B}\left(t\right) \qquad (2)$$

where $S_{v\text{-}neck}$ and $S_{a\text{-}neck}$ are coefficients representing sensitivities to body velocity and acceleration, respectively; and $\dot{B}$ and $\ddot{B}$ are body velocity and acceleration, respectively (see also Brooks and Cullen 2009). Additionally, neuronal responses to static changes in head-on-body position were quantified during periods (>2 s) for which the head was stationary and oriented at different positions relative to the body. For each neuron, the slope of the regression between head position and average firing rate provided an estimate of the neuron's static neck sensitivity.

Finally, we described each unit's response during combined vestibular and proprioceptive stimulation evoked by both passive and active head-on-body rotations (i.e., the combined condition, Fig. 1, *C* and *D*) using the equation:

$$\hat{fr}\left(t\right) = b + \left(S_{v\text{-}vest} + S_{v\text{-}neck}\right)\dot{HB}\left(t\right) + \left(S_{a\text{-}vest} + S_{a\text{-}neck}\right)\ddot{HB}\left(t\right) \qquad (3)$$

Note that because in this condition neck proprioceptive and vestibular sensitivities cannot be dissociated (i.e., head movement = head-on-body movement), they are estimated as a single coefficient. The estimated coefficient for a given neuron was then compared with that predicted based on the same neuron's sensitivity to vestibular and proprioceptive stimulation during whole-body rotation (*Eq. 1*) and body-under-head rotations (*Eq. 2*), respectively. This "summation model" provided a prediction of a neuron's response during combined stimulation based on the sum of its vestibular and neck sensitivities measured when each stimulus was delivered separately. We compared the ability of the summation model and a model based solely on the neuron's response to vestibular stimulation (i.e., *Eq. 1*, termed the "vestibular model") to describe neuronal responses during combined stimulation.

The goodness of fit of the data to each model was quantified by computing the variance-accounted-for {VAF = 1 − [var (mod − fr)/var(fr)], where mod represents the modeled firing rate, and fr represents the actual firing rate}. The VAF in linear models is equivalent to the square of the correlation coefficient (R^2), such that a model with a VAF of 0.64 provides as good a fit to the data as a linear regression analysis that yields a correlation coefficient of 0.80 (Cullen et al. 1996). The number of samples (N) for each VAF computation was substantive, since the time series data were sample at 1 kHz, and analysis was performed on 40 s of data (i.e., 20 cycles, 0.5-Hz rotation). Note that only data for which the firing rate was >10 spikes/s were included in the optimization to prevent fitting a given neuron's response during epochs where it was driven into cut-off.

Statistical analysis. All results were imported into Systat 10.0 software (SPSS, Chicago, IL) for statistical analysis. Normality of the distributions was determined using one sample Kolmogorov-Smirnov tests, with significance set at $P = 0.05$. If the distribution of the parameter was deemed normal using the Kolmogorov-Smirnov test and each sample included at least 15 values, statistical comparisons between numerical values were done through parametric test; two-by-two comparisons between cell groups were performed using Student's *t*-test. Otherwise, nonparametric tests with the threshold for significance set at $P = 0.05$ were done. Two-by-two comparisons between cell groups were performed using the Mann-Whitney *U*-test. All results are reported as means ± SE.

RESULTS

The neurons in our sample ($n = 30$) were modulated in response to vestibular stimulation and were insensitive to eye movements, consistent with VO neurons previously described in the alert mouse (Beraneck and Cullen 2007) and primate (Cullen and McCrea 1993; McCrea et al. 1999; Scudder and Fuchs 1992) under comparable head-restrained conditions. First, as is illustrated in Fig. 2 (*left* column), neurons encoded vestibular information during sinusoidal yaw rotations about an earth vertical axis. The three example neurons were robustly modulated in response to sinusoidal rotations at 0.5 Hz (±40°/s) [gains and phases (relative to velocity) = 0.15, 0.24, and 0.16 (spikes/s)/(°/s), and 9, −5, and −38°s, respectively] and thus had vestibular sensitivities similar to those described by Beraneck and Cullen (2007). Because passive rotation elicited a compensatory eye motion response, neuronal responses were also characterized during the static eye position paradigm (see METHODS) to confirm the lack of eye-movement-dependent modulation. In addition, all neurons were unresponsive to eye position during saccades and the quick phases of vestibular nystagmus. Depending on whether a neuron's firing rate increased during ipsilaterally ($n = 18$) or contralaterally ($n = 12$) directed vestibular stimulation, neurons were classified as type I or type II, respectively.

The majority of neurons respond to passive proprioceptive as well as vestibular stimulation. We next addressed whether the same mouse VN neurons that respond to vestibular stimulation also respond to the activation of neck proprioceptors. To explicitly test this proposal, we recorded the responses of the same neurons during a paradigm in which neck proprioceptor stimulation was delivered in isolation. The *right* column of Fig. 2 illustrates the responses recorded from the three example neurons while we sinusoidally rotated the mouse's body beneath its earth-stationary head (0.5 Hz, ±40°/s). A minority of neurons ($n = 9/30$) were insensitive to neck proprioceptor stimulation (Fig. 2*A*), whereas the remaining 70% ($n = 21/30$) showed significant modulation (Fig. 2, *B* and *C*). Accordingly, based on their sensitivities to vestibular (i.e., whole body rotations) and/or neck proprioceptive stimulation (i.e., body-

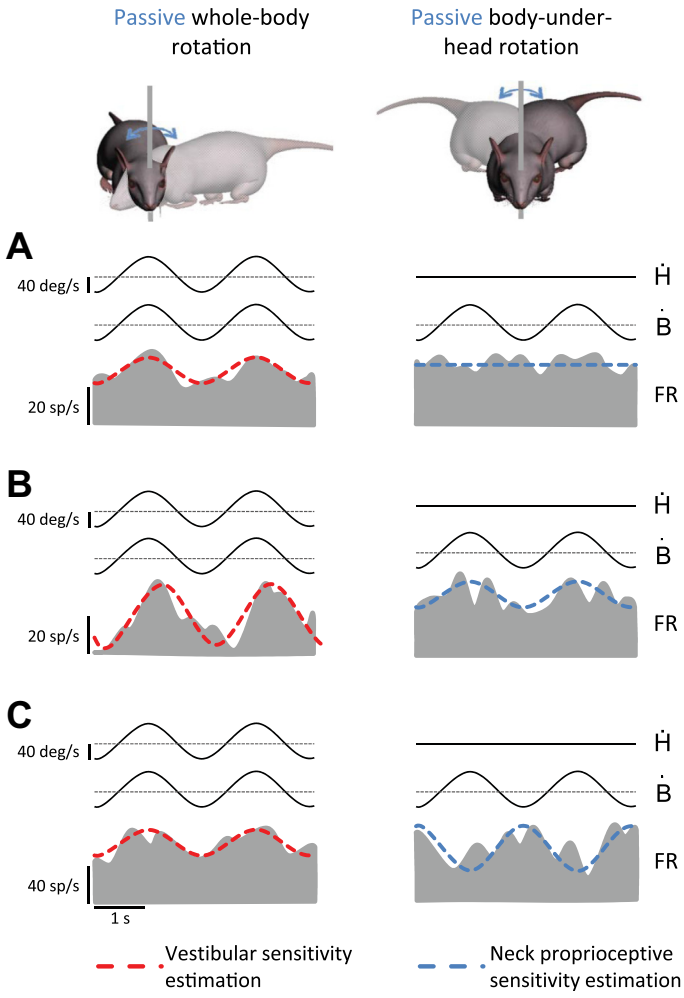

Fig. 2. Activity of example unimodal (*A*), bimodal antagonistic (*B*), and bimodal agonistic (*C*) neurons during vestibular (*right* column) and proprioceptive (*left* column) stimulation paradigms. Neck proprioceptor stimulation was applied by rotating the body under the head. Note that unimodal neurons are not modulated during this paradigm, while both classes of bimodal neurons show robust responses. Thick lines overlaying the firing rate (FR) represent a model based on estimated resting discharge and head [red (*Eq. 1*); *right* column], or body [blue (*Eq. 2*); *left* column] movement sensitivities.

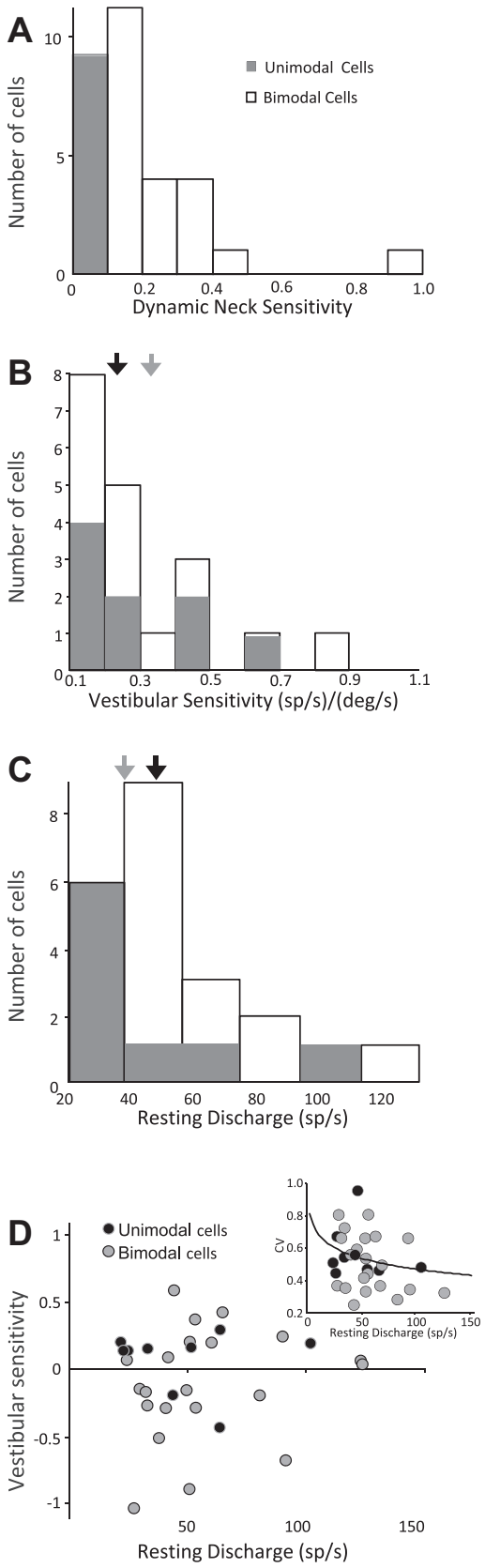

under-head rotations), neurons were categorized as either unimodal (responding only to vestibular stimulation) (Fig. 2*A*) or bimodal (Fig. 2, *B* and *C*). Notably, this distinction is further motivated by the distribution of neuronal dynamic and static neck sensitivities (Figs. 3 and 4, respectively), as well as by prior investigations in cat and monkey (Gdowski and McCrea 2000; Kasper et al. 1988; Sadeghi et al. 2009). The proprioceptive responses of the two example bimodal neurons were characterized by gains and phases (relative to velocity) of 0.15 and 0.25 (spikes/s)/(°/s) and 48 and −77°s, respectively, and were representative of the neurons in our sample in that they had comparable modulation in response to proprioceptive and vestibular stimulation.

Figure 3 summarizes the population data for both groups of neurons. Figure 3, *A* and *B*, shows the distributions of neuronal neck and vestibular sensitivities, respectively. During body-under-head rotation, the mean response modulation of the population of bimodal neurons was 0.25 ± 0.40 (spikes/s)/(°/s). As expected, the average modulation of unimodal neurons was not significantly different from zero (Fig. 3*A*) ($P >$ 0.40). In contrast, the vestibular sensitivities of both groups of neurons were comparable (Fig. 3*B*) [0.23 ± 0.05 and 0.34 ± 0.06 (spikes/s)/(°/s) for unimodal and bimodal cells, respectively; $P = 0.22$]. Each neuron's resting discharge (Fig. 3*C*) and discharge regularity (Fig. 3*D*, *inset*) quantified by CV (see METHODS) were also determined in the absence of vestibular or neck stimulation with the animal's head centered on its body. On average, the resting discharges of unimodal and bimodal neurons were similar (Fig. 3*C*: unimodal: 40.4 ± 9.9 spikes/s; bimodal: 53.2 ± 4.7 spikes/s; $P = 0.11$) and did not vary as a function of vestibular sensitivity (Fig. 3*D*). For the entire population, the relationship between neuronal discharge regularity (CV) and resting rate (Fig. 3*D*, *inset*) was comparable to that previously described for mouse VO neurons (Beraneck and Cullen 2007). Moreover, we observed no difference in this relationship for unimodal vs. bimodal neurons (unimodal: 0.61 ± 0.06; bimodal: 0.53 ± 0.05; $P = 0.33$), and additionally found that the regularity of unimodal neurons remained unchanged from resting values during neck proprioceptor stimulation ($P = 0.2$).

To further explore the origin of the neck-relatedsignals encoded by mouse bimodal VN neurons, we next tested whether neurons showed responses to static changes in head

Fig. 3. Distribution of neck proprioceptive and vestibular sensitivities, and basic discharge parameters of mouse vestibular nuclei (VN) neurons. *A*: distribution of neck proprioceptive sensitivities. Classification of neurons was done according to the sensitivity of their discharge to body-under-head rotation. Cells with no neck proprioception sensitivity [i.e., <0.1 (spikes/s)/(°/s)] were classified as unimodal neurons ($n = 9$), whereas cells with a proprioception sensitivity >0.1 (spikes/s)/(°/s) were classified as bimodal neurons ($n = 21$). *B*: distribution of vestibular sensitivities determined during whole-body rotation. Black and gray arrows indicate the mean values for unimodal and bimodal neurons, respectively. *C*: distribution of resting discharge rate for the entire population. Black and gray arrows indicate the mean values for unimodal and bimodal neurons, respectively. *D*: lack of relationship between vestibular sensitivity and the resting rate. No relationship was observed between neuronal sensitivities to vestibular stimulation and resting FRs for either unimodal and bimodal neurons. *Inset*: relationship between the coefficient of variation and the resting rate for unimodal neurons (black circles) and bimodal neurons (gray circles). Note, the curve is fit across the entire neuronal population since no significant differences were seen between unimodal and bimodal neurons.

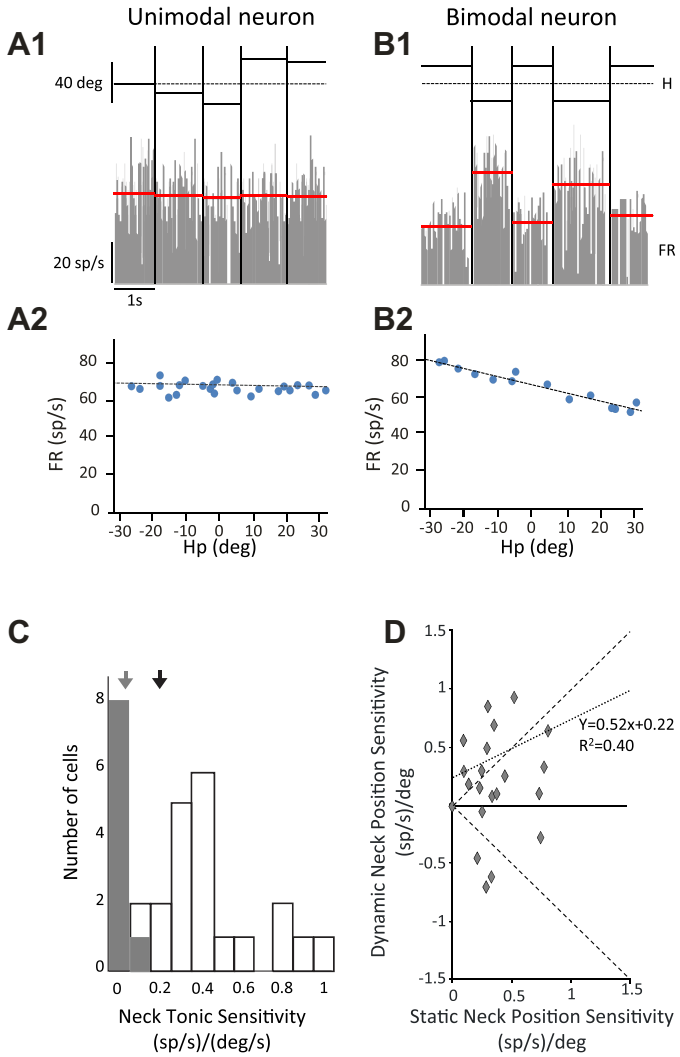

Fig. 4. Bimodal VN neurons are sensitive to changes in static neck position. *Top* row: activity of example unimodal and bimodal neurons recorded with the head stationary at different positions relative to the body (*A1* and *B1*, respectively). Because only time intervals during which the head and body were stable in space are displayed, time is discontinuous between each vertical line. *Middle* row: average FR is correlated with static head position (Hp) for the bimodal neuron (*B2*) but not for the unimodal neuron (*A2*), and neurons at different positions do not change with neck position; error bars represent ± standard error. *Bottom* row: distribution of static neck position sensitivity for the population of bimodal neurons (*C*), where the gray arrow indicates the mean value. Overall, the static neck sensitivity of a given neuron was not well correlated with its response to dynamic neck stimulation (*D*). Dashed lines represent unity lines. Static neck position sensitivity from dynamic segments and the static neck position signal were however correlated for positive values, as represented by the solid line (slope = 0.52, *y*-intercept = 0.22, and $P = 0.01$).

orientation relative to the body, as well as the responses to dynamic changes described above (Fig. 2, *right* column). We analyzed recordings from neurons in the absence of vestibular stimulation during intervals in which the body was rotated relative to the head and then held stationary over a range of ±20°. The responses of the example neurons shown in Fig. 4, *A1* and *B1*, are representative of the unimodal and bimodal neurons in our sample. Whereas the unimodal neuron was unresponsive to changes in the static positions of the head relative to the body (Fig. 4*A2*; $P = 0.11$), the bimodal neuron's response displayed a strong dependence on static head position (Fig. 4*B2*; slope = 0.4, $P < 0.001$). Similar results were obtained for 95% (i.e., all but one neuron) of our sample of bimodal neurons [mean sensitivity: 0.44 ± 0.09 (spikes/s)/(°), Fig. 4*C*], while none of our unimodal neurons showed significant sensitivity to static neck stimulation.

Accordingly, bimodal neurons were distinguished by their sensitivity to static changes in head orientation (i.e., position relative to the body), as well as sensitivity to dynamic stimulation of neck proprioceptors. To better understand the relationship between these signals, we compared the magnitude of the static response sensitivity and the sensitivity to dynamic neck proprioceptive stimulation recomputed relative to position. This computation allowed us to compare sensitivities expressed in the same units (spikes/s)/(°), to test whether responses to neck sensitivity are similar in magnitude in both conditions, and/or whether they are systematically correlated across neurons. When both sensitivities were ipsilateral (i.e., positive values), there was a small but significant correlation between each measure (Fig. 4*D*, slope = 0.52, *y*-intercept = 0.22, $R^2 = 0.40$ and $P = 0.01$). Thus our findings suggest that the static head orientation signal observed in VN may arise, at least in part, from the integration of a given neuron's dynamic proprioception signal.

Bimodal neurons encode the linear summation of the vestibular and neck sensitivities during passive motion. We next addressed the question of how VN neurons in mice combined vestibular and neck proprioceptive information in conditions where these inputs are not delivered in isolation. For instance, whenever the head moves relative to the body, vestibular sensors and neck proprioceptors will be simultaneously activated. To address this question, we tested the hypothesis that these two inputs sum linearly during combined stimulation in mice. We first computed the vestibular response vector defined by the gain (length) and phase (angle) of the neural response to passive whole body rotation, for each neuron in our unimodal and bimodal populations neurons (arrows, Figs. 5, *A–C*). We then computed the proprioceptive response vector, defined by the gain (length) and phase (angle) of the neural response to passive body-under-head rotation, for each biomodal neuron. Notably, this second analysis revealed that bimodal mouse VN neurons could be further subdivided into two groups: antagonistic neurons which were characterized by oppositely directed vestibular and neck proprioceptive sensitivities ($n = 10/21$, 48%) and agonistic neurons for which the preferred directions of vestibular and neck proprioceptive stimulation were the same ($n = 11/21$, 52%). Note, the example bimodal neurons shown in Fig. 2, *B* and *C*, show antagonistic and agonistic responses, respectively.

The polar plots in Fig. 5, *A–C*, show the vestibular response vectors (*left*) and proprioceptor response vectors (*right*) for each group of neurons [unimodal (Fig. 5*A*), bimodal antagonistic (Fig. 5, *B1* and *B2*), and bimodal agonistic (Fig. 5, *C1* and *C2*)]. The thick red and blue arrows represent average neuronal responses to vestibular and proprioceptive stimuli applied in isolation (n.b., neck movement sensitivity vectors were not associated with unimodal neurons, since these neurons were insensitive to neck rotations). The lengths and directions of average vestibular response vectors were comparable for all groups of neurons ($P > 0.1$). In addition, there was no difference in the magnitude of the proprioceptive response vectors of bimodal antagonistic and agonistic neurons ($P >$

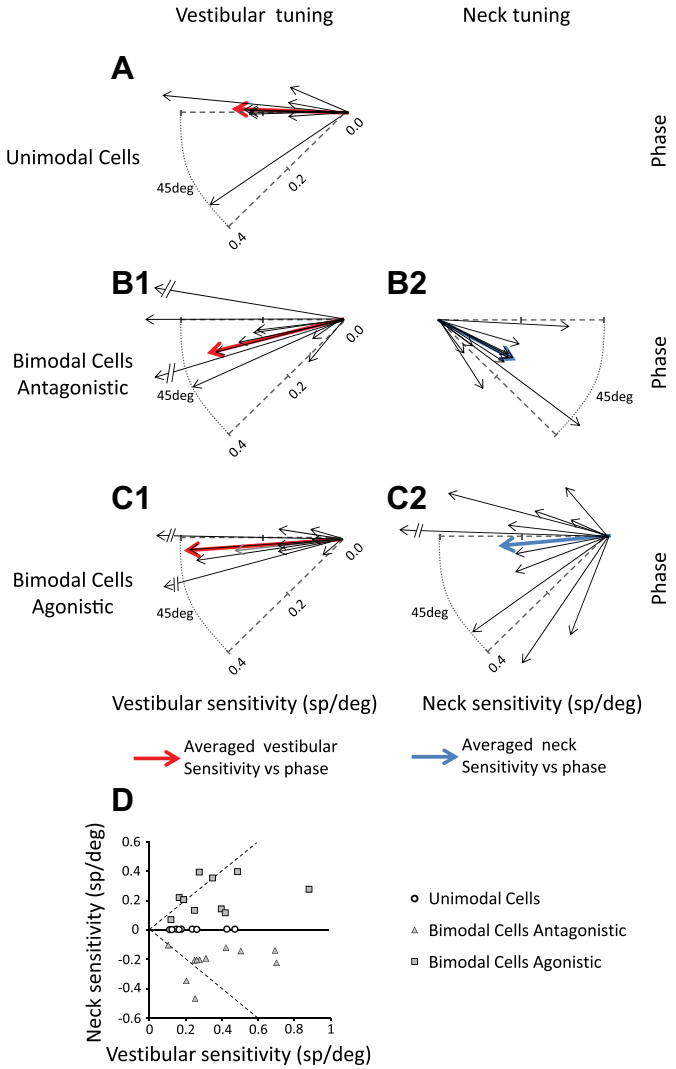

Fig. 5. Comparison of neuronal vestibular and neck proprioceptive sensitivities. *A*, *B*, and *C*: polar plots of the vestibular (*left*) and neck proprioceptive (*right*) sensitivities of unimodal (*A*; $n = 9$), bimodal antagonistic (*B*; $n = 11$), and bimodal agonistic (*C*; $n = 10$) neurons. The length of the arrows indicates the sensitivity, and the angle represents the phase of the response. Superimposed red arrows are mean population vectors for vestibular, and superimposed blue arrows are mean population vectors for neck proprioceptive stimulation. *D*: vestibular vs. neck sensitivity for unimodal, bimodal agonistic, and bimodal antagonistic neurons. Dashed lines represent unity line.

0.1). Overall, however, the magnitude of the average vestibular response vector for our entire population of bimodal neurons (i.e., the combined population of antagonistic and agonistic cells) was significantly larger ($P < 0.05$) than that of the comparable proprioceptive response vector (mean vector magnitude for all bimodal neurons, 0.34 ± 0.05 vs. 0.24 ± 0.04). This comparison is made for each neuron in Fig. 5*D*.

Note that, for the head on body movements made in everyday life, the resulting vestibular and proprioceptive inputs would be antagonistic since the motion of the head relative to space (i.e., vestibular stimulation) results in an equal and opposite motion of the body relative to the head (i.e., proprioceptive stimulation). Thus, if bimodal neurons linearly sum their vestibular and neck proprioceptive sensitivities during such combined stimulation, antagonistic neurons should show minimal modulation (since the two inputs would effectively cancel out when combined), whereas those of bimodal agonist neurons would show enhancement relative to conditions where either stimulus is applied alone, as a result of the combined stimulation. To test this proposal, we next recorded the response of the same neurons while the head was rotated so that it moved relative to an earth-stationary body (i.e., head-on-body rotations). The responses of three example neurons (the same neurons in Figs. 2 and 4) are shown in Fig. 6. These neurons are typical in that the summation of their neuronal sensitivities to head and neck rotation when applied alone predicted responses to head-on-body rotations. Specifically, the example unimodal neuron (Fig. 6*A*) responded robustly with a gain and phase that was not different from that measured during pure vestibular stimulation. Additionally, the modulation of both example bimodal neurons was well described by the sum of their vestibular and proprioceptive sensitivity measured when each stimulus was delivered separately (summation model; solid green line). Finally, as predicted, the modulation of the example antagonistic bimodal neuron (Fig. 6*B*) was greatly attenuated when the head was rotated on the body compared with when the head and body were rotated together in space (vestibular model; red line), whereas the modulation of the agonistic bimodal neuron was enhanced (Fig. 6*C*).

To quantify our ability to predict responses across the population of VN neurons, we computed the VAF (see METHODS) provided by the optimized best fit to neuronal responses (i.e., "estimate", Fig. 6) and the VAF provided by the linear summation model (i.e., "vestibular and neck prediction", Fig. 6). First we established that estimated best fit accounted for ~23, 18, and 36% of firing rate variance of unimodal, antagonist, and agonistic neuronal responses, respectively. We next found that the linear summation model described the responses of neurons in each group nearly as well. Specifically, the linear summation model accounted for 92% as much variance as the estimated best fit {population averages for all neurons ($n = 30$); 0.25 ± 0.04 for the best estimate vs. 0.23 ± 0.03 for the linear prediction [subgroups: unimodal ($n = 9$) 0.23 ± 0.05 vs. 0.21 ± 0.05; antagonist ($n = 10$) 0.18 ± 0.05 vs. 0.17 ± 0.04; and agonist ($n = 11$) 0.36 ± 0.05 vs. 0.32 ± 0.05]}. Notably, as shown below, the linear model's ability to describe responses to passive head-on-body motion is in striking contrast to what was observed for responses to active head-on-body motion (see Fig. 8).

Next we compared, on a neuron-by-neuron basis, the estimated and predicted head-on-body gains for all the unimodal (Fig. 7*A*), bimodal antagonistic (Fig. 7*B*), and bimodal agonistic neurons (Fig. 7*C*) neurons in our sample. For the two latter cell groups, sensitivities predicted by the linear sum of vestibular and neck sensitivities and the actual measured sensitivities to head-on-body velocity were comparable (combined model; gray symbols); the slope of the lines fitting these data was not different from unity ($P = 0.16$ paired *t*-test, $n = 10$ and $P = 0.66$ paired *t*-test, $n = 11$, respectively). To further this analysis, we also compared each neuron's sensitivity to vestibular stimulation in isolation (vestibular model; open symbols) and the actual measured sensitivities to head-on-body velocity. Note that this model was identical to the linear summation model for unimodal neurons and thus provided a prediction equivalent to the combined model ($P = 0.44$ paired *t*-test, $n = 9$). In contrast, the vestibular model overpredicted the responses of bimodal antagonistic cells (slope = 1.2) and under-

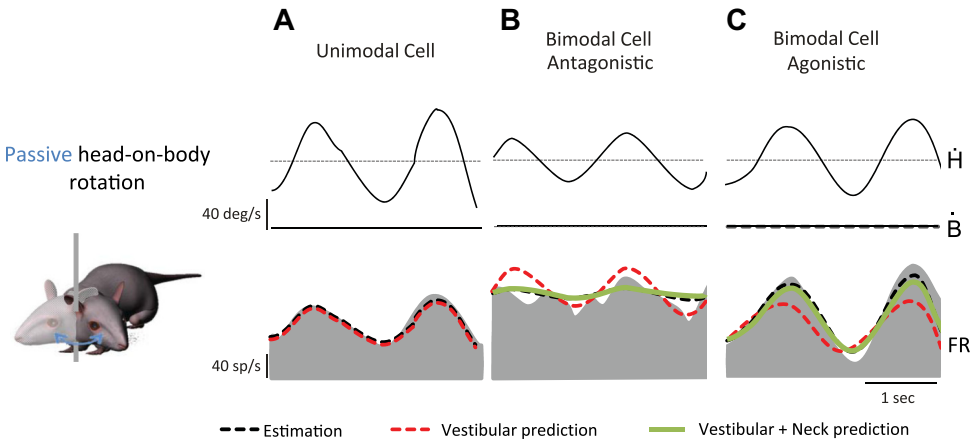

Fig. 6. Activity of example unimodal (*A*), bimodal antagonistic (*B*), and bimodal agonistic neurons (*C*) (Fig. 1) during passive head-on-body rotations. Note that the unimodal neuron's activity (*A*) could be predicted based on a summation of its neck proprioceptor and vestibular sensitivities (solid green line) or by its vestibular sensitivity alone (solid red line), since the two models are equivalent. In contrast, the responses of the both bimodal neurons (*B* and *C*) were not well predicted based solely on their vestibular sensitivity (solid line), but rather were better modeled by a prediction based on the summation of vestibular and neck proprioceptive sensitivities [solid green line (see METHODS)].

predicted the responses of bimodal agonistic neurons (slope = 0.49) as expected based on our initial hypothesis.

Neurons do not encode the linear summation of the vestibular and neck sensitivities during active motion: instead dynamic responses are suppressed. During the generation of active head-on-body movements, not only are the vestibular sensors and neck proprioceptors simultaneously activated, but also a motor command is produced to move the head. To understand how self-motion information is encoded by the mouse vestibular system during active movements, we next investigated VN responses when mice generated their own head-on-body motion. If responses can be predicted based on the linear summation of the vestibular and neck sensitivities, then we would expect results similar to those shown in Fig. 7 for passive head-on-body motion. Responses were analyzed for all neurons characterized above during passive paradigms for which the isolation remained robust during active movement (n = 25/30). Recall that, in the passive condition, two classes of head-on-body rotation stimuli were applied: *1*) sinusoidal stimuli (i.e., Fig. 6*A*); and *2*) stimuli designed to mimic those actively generated by the mouse (Fig. 8, *A2* and *B2*). We found that all groups of neurons responded similarly in both conditions. Specifically, neuronal sensitivities to passive head-on-body motion were comparable regardless of whether the applied rotation was sinusoidal or "active-like" (P = 0.42 paired t-test, n = 25).

Figure 8, *A* and *B*, shows the responses of an example bimodal neuron (agonistic) and unimodal neuron during passive vestibular stimulation (i.e., passive whole body rotation, Fig. 8, *A1* and *B1*), combined passive vestibular and proprioceptor stimulation (i.e., the "active-like" passive head-on-body rotation, Fig. 8, *A2* and *B2*), and active head-on-body rotations (Fig. 8, *A3* and *B3*). For each neuron, we first assessed whether the linear summation of its vestibular and neck-related sensitivities measured during passive whole body rotation and passive body under head rotation, respectively (*Eq. 3*), could predict its modulation in the active condition. As is shown for both example neurons, the linear prediction provided a poor fit of neuronal responses in the active condition (solid green line) compared with an estimate in which coefficients were independently optimized (black solid line). Thus this finding contrasts with the results described above, in which the same linear prediction provided a good fit for both neurons during passive head-on-body movements.

To quantify this finding, we computed the goodness of the fits (VAF, see METHODS) provided by the linear summation prediction model vs. best estimate and confirmed that the former did not provide a good fit to neuronal firing rates in the active condition. Overall, similar to the passive condition, optimized fits to the active data accounted for ~25% of the firing rate variance. In contrast, the VAF provided by the linear summation prediction was actually negative for responses to active head-on-body motion. Thus, in the active condition, the linear summation prediction model actually provided a worse fit than would have been obtained by simply fitting a mean to the data [population averages: unimodal (n = 7), 0.25 ± 0.05 vs. −1.08 ± 0.54; antagonist (n = 9), 0.25 ± 0.04 vs. −0.58 ± 0.47; and agonist (n = 9), 0.26 ± 0.05 vs. −8.16 ± 5.45; for all neurons 0.25 ± 0.04 vs. −3.45 ± 0.47, $P < .00001$]. Accordingly our quantitative analysis of the goodness of fit of the linear model prediction in the active motion condition establishes that the linear summation model cannot predict neuronal responses. Notably, the gain of response modulation during active head movements (relative to the head velocity) was consistently significantly less than that predicted based on the linear summation of vestibular and neck sensitivities obtained during passive rotations [−0.03 ± 0.04 vs. 0.33 ± 0.05 (spikes/s)/(°/s), paired t-test, $P < 0.01$, n = 25].

A comparison of the estimated and predicted sensitivities during active head movements on a cell-by-cell basis is shown in Fig. 9 for unimodal (Fig. 9*A*), bimodal antagonistic (Fig. 9*B*) and bimodal agonistic (Fig. 9*C*) neurons. For each neuron class, almost all the data points fall below the unity line (dashed line labeled "linear prediction"), indicating that estimated sensitivities were less than expected based on the linear summation of vestibular and neck sensitivities to passive motion. Thus, unlike the passive condition, the response of VN neurons cannot be predicted by the simple addition of vestibular and neck signals during active head-on-body movements. In general, the passive prediction overestimated the active signal, consistent with an attenuation of sensory-related responses during self-produced motion.

Biomodal neurons encode static head orientation signals in both active and passive conditions. Surprisingly, however, we found that both antagonistic and agonistic bimodal neurons continued to robustly encode static changes in head orientation (i.e., position relative to the body) between active movements.

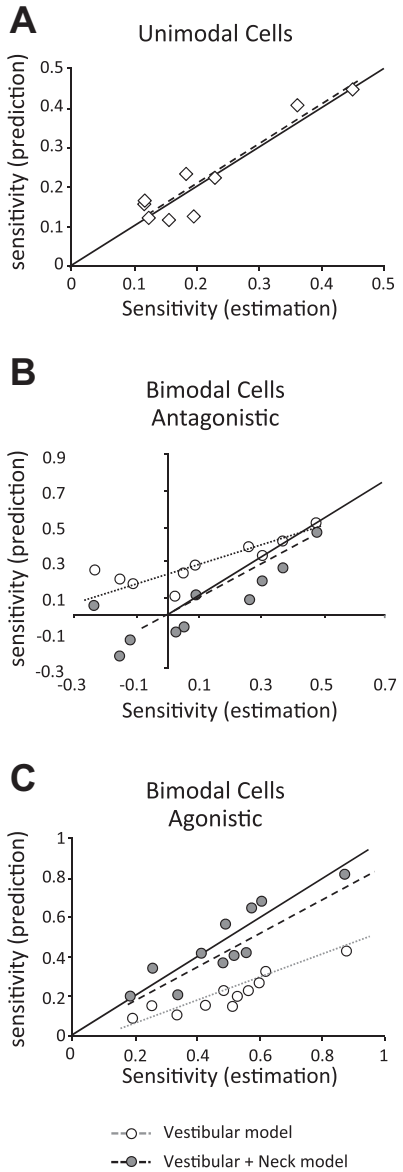

Fig. 7. Linear summation of the vestibular and neck sensitivities well predicts neuronal responses in passive conditions. *A*: comparison of estimated and predicted sensitivities of unimodal neurons to head-on-body rotations. The open diamonds represent the prediction of the vestibular model. *B* and *C*: comparison of estimated and predicted sensitivities of bimodal antagonistic (*B*) and agonist (*C*) neurons to head-on-body rotations. The filled gray circles represent comparison between response sensitivity and the combined model prediction. The open circles represent comparison between response sensitivity and the vestibular model prediction. Note that estimated and predicted head-on-body velocity sensitivities using the summation model were comparable for the bimodal neurons (*B* and *C*: slope was 0.94 for bimodal antagonistic neurons and 0.86 for bimodal agonistic neurons, respectively). Solid line indicates line of unity slope.

Notably, this active orientation signal has not been previously described in the VN of any species. We computed each neuron's sensitivity to changes in head orientation produced by active rotations and compared this value to the same neuron's sensitivity to head orientation following passive head rotations (i.e., Fig. 4). Figure 9*D* compares the static orientation sensitivity in both conditions. The similarity of the sensitivity estimated between the two conditions is shown by the slope of the line fitted to the data (regression slope = 1.0), which was not different from unity ($n = 18$, $P = 0.63$). Thus, taken as a population, bimodal neurons encoded comparable information about head orientation relative to the body following active and passive motion. The implications of this result are further considered in the discussion.

DISCUSSION

During everyday activities, proprioceptive and motor-related signals as well as vestibular inputs provide information about an animal's movement through the world. The mouse has become an important model system for studying the cellular basis of learning and coding of heading by the vestibular system, yet prior to this study it was not known how its early vestibular pathways encode self-motion information under natural conditions for which these other self-motion cues are present. Recordings were made in alert behaving mice at the first central stage of vestibular processing, focusing on the neurons that control posture and project to higher-order structures involved in the estimation of self-motion (reviewed in Cullen 2012). The majority of neurons were sensitive to passive stimulation of proprioceptive as well as vestibular receptors. When both stimuli were applied concurrently, a given neuron's modulation was predicted well by the linear sum of its sensitivity to each stimulus when applied in isolation. In contrast, when comparable dynamic stimulation was the result of self-generated motion, neuronal responses were attenuated relative to those predicted by this linear model. Importantly, however, we also made the striking discovery that bimodal neurons encode a static neck position following active as well as passive head movements. Notably, this signal remained robust (i.e., was not attenuated) for active compared with passive movements. Taken together, our findings show that proprioceptive and motor-related signals are combined with vestibular information at the first central stage of vestibular processing in mice. Since the descending projections of these neurons likely mediate spinal postural reflexes such as the vestibulocollic reflex, these results suggest that vestibular reflexes are modulated in a behaviorally-dependent manner. Moreover, we suggest that our results have important implications for understanding the genesis of the internal representation of HD by the HD cells located throughout the classical Papez circuit, which likely reflect the integration of multimodal signals (vestibular, proprioceptive, motor efference copy, etc.).

Vestibular signals carried by VN neurons. Our findings are consistent with the previous studies that have characterized the responses of VO neurons in mouse VN (Beraneck and Cullen 2007), providing further evidence that the average head velocity sensitivity of neurons is ~0.3–0.4 (spikes/s)/(°/s) for rotation at 0.5 Hz. Overall, these neurons show relatively low sensitivities to head velocity compared with VN neurons in other species such as rabbit (Stahl and Simpson 1995), cat (Cheron et al. 1996; Escudero et al. 1992) or monkey (Cullen et al. 1993; Cullen and McCrea 1993). The lower sensitivities of mouse VN neurons, however, are consistent with the results of several recent studies establishing that mouse afferents are on average 3–4 time less sensitive to head velocity than are monkey afferents (Lasker et al. 2008; Yang and Hullar 2007). Together, these findings suggest the coadaptation of the firing properties of mouse vestibular afferents and central neurons similar to that proposed in the frog (Pfanzelt et al. 2008).

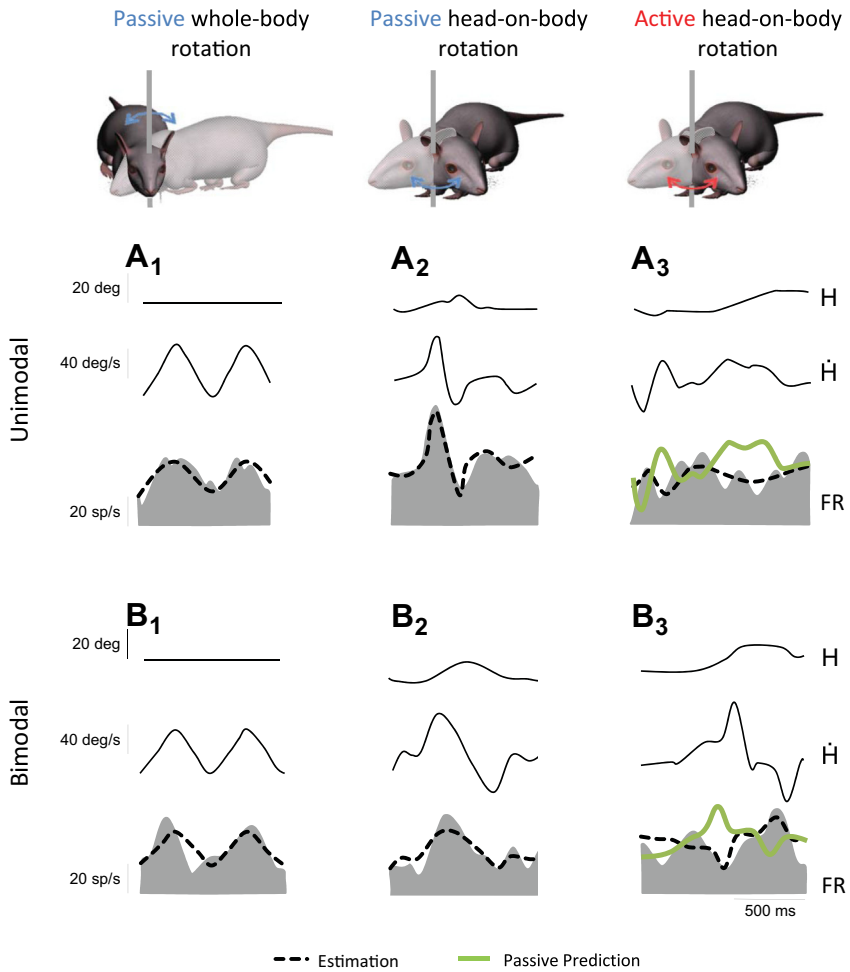

Fig. 8. Activity of an example unimodal (*A*) and bimodal (*B*) neuron during active head-on-body rotations. Note that during active movements neither the unimodal nor bimodal neuron's activity (*A3* and *B3*) could be predicted based on the neuron's sensitivities to passive stimulation vestibular (i.e., response during passive whole body rotation; *A1* and *B1*) and/or passive proprioceptive stimulation (i.e., response during passive head-on-body rotations; *A2* and *B2*). This prediction is indicated by the superimposed solid green line labeled passive prediction. Notably, this finding contrasts with the result shown in Fig. 6 for passive head-on-body rotations, for which the summation model provided a good estimate of neuronal FR for both unimodal and bimodal neurons.

The functional significance of relatively lower discharges of mouse vestibular neurons remains to be determined. One possible explanation might be that neuronal responses are matched to the specific mechanical constraints of the reflexes that the mouse sensory-motor pathways have evolved to control. For instance, the control of eye movements or posture could have a "lower neural cost" in mice since the inertia load is less than in larger species. However, a recent report that the sensitivities of mouse extraocular motoneurons lie between those of the monkey and rabbit (Stahl and Thumser 2012) does not support this idea. Alternatively, the relatively lower discharges of mouse vestibular neurons could reflect a limited need for behavioral and/or perceptual accuracy, suggesting that they might also encode less information (Borst and Haag 2001; Vinje and Gallant 2000). Indeed, our preliminary experiments suggest that mouse VO neurons encode substantially less information than do monkey neurons during self-motion (Jamali et al. 2010), suggesting evolutionary pressure adjusts performance to the minimum required for adequate function, which may differ across species (see Niven et al. 2007).

Neck proprioceptive signals are carried by VN neurons. The VN receive proprioceptive inputs via both monosynaptic projections from the contralateral central cervical nucleus (Sato et al. 1997) and direct projections from the cerebellum (Akaike 1983; Furuya et al. 1975; Noda et al. 1990; Robinson et al. 1994). Consistent with these projections, we found a significant percentage (70%) of mouse VO neurons were also sensitive to the dynamic activation of neck proprioceptors produced by passive body-under-head rotations (i.e., bimodal neurons). This finding is comparable to previous reports of vestibular-proprioceptive integration in decerebrate cats (Anastasopoulos and Mergner 1992; Boyle and Pompeiano 1981; Wilson et al. 1990), alert squirrel monkeys (Gdowski and McCrea 2000) and cynomolgus monkeys (i.e., *macaca fasicularis*) (Sadeghi et al. 2009), species in which at least 50% of neurons respond to passive stimulation of neck proprioceptors. However, in rhesus monkeys (*macaca mulatta*), neither VO nor other types of VN neurons (i.e., position-vestibular-pause and eye head neurons) respond to passive stimulation of the neck proprioceptors (Roy and Cullen 2001, 2002, 2003). It remains to be determined which of these species provides a better model for multimodal integration in the human brain.

We further found that mouse bimodal neurons in the VN are equally likely to respond to proprioceptive stimulation that is antagonistic or agonistic to their vestibular sensitivities. Similarly, the proprioceptive sensitivities of bimodal cat VN neurons are also antagonistic and agonistic in equal proportions (Anastasopoulos and Mergner 1992; Boyle and Pompeiano 1981), while neurons in squirrel and cynomolgus monkeys are characterized exclusively by antagonistic neck-related responses relative to their vestibular sensitivities (Gdowski and McCrea 2000, Sadeghi et al. 2009, respectively). Theoretically, the agonistic bimodal neurons observed in the mouse and cat

would function to enhance the head-on-body signal, whereas the antagonistic neurons would function to suppress this signal.

In the present study, we also discovered that most neurons in the VN are sensitive to static changes in neck position, such that they encode static head orientation relative to the body. Such a static neck position signal has been observed in the VN of cats (Anastasopoulos and Mergner 1992; Boyle and Pompeiano 1981; Wilson et al. 1990) and rats (e.g., Barresi et al. 2013), but not primates and, as discussed below, is likely to provide vital information to upstream structures for the computation of spatial orientation during active as well as passive self-motion.

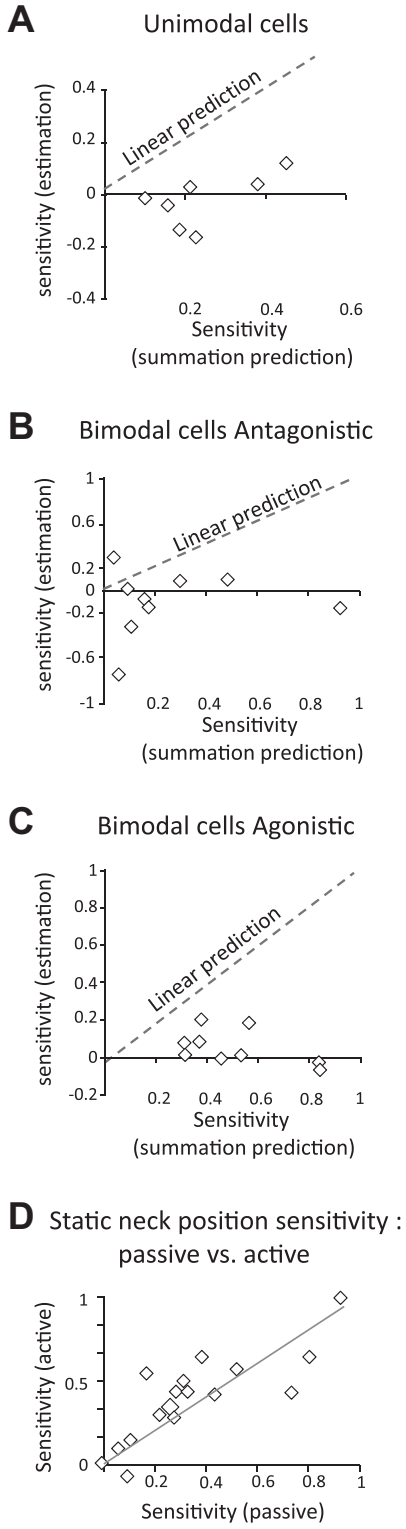

Fig. 9. Comparison of responses during active vs. passive movements. *A–C*: linear summation of the vestibular and neck sensitivities does not predict neuronal responses to dynamic active head movements. *A*: comparison of responses as estimated during active movements and predicted from passive movements of unimodal neurons ($n = 7$) to head-on-body rotations. *B*: comparison of responses as estimated during active movements and predicted from passive movements of bimodal antagonistic neurons ($n = 9$) to head-on-body rotations. *C*: comparison of responses as estimated during active movements and predicted from passive movements of bimodal agonistic neurons ($n = 9$) to head-on-body rotations. *D*: bimodal neurons show similar responses to changes in static Hp for active vs. passive movements for all bimodal neurons ($n = 18$, $P = 0.63$). Plot illustrates comparison of neck static sensitivities of bimodal neurons in the two conditions.

Multimodal integration: convergence of vestibular, proprioceptive, and motor-realted signals. When neurons in the present study were tested during combined neck proprioceptive and vestibular stimulation resulting from passive head-on-body rotations, their responses could be predicted based on the sum of their vestibular sensitivity during passive whole body rotation and neck sensitivity during passive rotation of the body under head, consistent with previous studies in anesthetized/decerebrate cats (Kasper et al. 1988) and alert squirrel and cynomolgus monkeys (Gdowski et al. 2001; Sadeghi et al, 2009).

In contrast, the summation of vestibular and neck sensitivities (estimated in passive rotation paradigms) did not reliably predict the responses of these VN neurons to active head motion. Instead, responses showed dramatic attenuation, comparable to that previously observed in monkey (Gdowski and McCrea 2000; Roy and Cullen 2001; Sadeghi et al. 2009). Importantly, these neurons are located within a first-order sensory nucleus that receives direct input from the vestibular afferents. Thus neurons in this nucleus, including interneurons (Malinvaud et al. 2010), are modulated by vestibular stimulation during passive head motion. It has been proposed that a copy of the motor efferent command signal is used to selectively cancel vestibular input carried by the afferents during active head rotations in monkeys (e.g., Roy and Cullen 2004, Sadeghi et al. 2009). We propose that a similar mechanism functions to suppress self-generated vestibular input during active head movements in lower mammalian species, including mice.

Finally, perhaps the most striking and important result of the present study was our finding that the static head-on-body sensitivity of mouse neurons, initially observed in response to passively applied changes in head orientation, remains present and robust for active movements. This result has not been reported in previous studies of central vestibular neurons during self-generated movements, which to date have only been performed in primates. As reviewed above, the VN in primate species studied to date do not encode a static neck position signal even in the passive condition, and as such there can be no persistence of this signal in the active movement condition. Thus the present study provides the first report of a static neck position signal on neurons in the VN for active motion. VN neurons are known to encode static neck information during passive motion in other species (e.g., cats: Anastasopoulos and

Mergner 1992; Boyle and Pompeiano 1981; Wilson et al. 1990; and rats: Barresi et al. 2013). Thus we speculate that VN neurons in these species will similarly encode a comparable static neck signal during active motion.

It is likely that divergence observed in the integration of sensory information in early vestibular processing across species has evolved as a result of variations across species in behavior as well as habitat. While both monkeys and mice are quadrupeds, monkeys can adopt bipedal postures in their natural habitat and frequently explore their environment with voluntary head-on-body movements termed gaze shifts (Freedman and Sparks 1997, 2000; Goossens and Van Opstal 1997). These coordinated eye-head gaze shifts allow the precise alignment of the axis of gaze to ensure clear binocular vision in monkeys, which are frontal-eyed animals with a retina specialized for high-acuity vision (fovea). In contrast, mice are lateral-eyed afoveates for which gaze coordination is less precisely controlled (see discussion in Stahl et al. 2006). Head and body motion are typically more closely linked in mice, and we speculate that the static neck sensitivity observed during active and passive motion in mouse serves to enhance the efficacy of mechanisms that support the stabilization of the head relative to the body (e.g., Baker 2005; Takemura and King 2005), a strategy developed to meet the requirements of its behavioral repertoire. In contrast, such coupling would be potentially detrimental in monkeys, which more commonly exercise voluntary control over the neck musculature. Additionally, there is most likely greater segregation between vestibulo-spinal and vestibulo-ocular reflexes in species such as primates vs. mice. For example, Boyle, McCrea, and colleagues (Boyle et al. 1996) reported a lower percentage of eye movement sensitive VN neurons with collaterals to spinal cord in the primate compared with cat.

Implications for the observed integration of signals. What functional role does the multimodal integration observed in early vestibular processing play in mice? While the vestibular sensors encode the motion of the head relative to space, neck proprioceptors provide information concerning the orientation of the head relative to the body. By combining these two sensory inputs, neurons can create a representation of body movement and/or convert vestibular information from a head-centered into a body-centered reference frame (Brooks and Cullen 2009; Kleine et al. 2004; Shaikh et al. 2004), computations required to ensure the maintenance of posture and balance during daily activities. The descending projections of neurons that were the focus of the present study likely mediate spinal postural reflexes such as the vestibulocollic reflex (Boyle 1993; Boyle et al. 1996; Wilson et al. 1990). Our results thus suggest that vestibular reflexes are modulated in a behaviorally-dependent manner; the sensory-motor integration observed in the VN likely suppresses the efficacy of reflexive descending spinal pathways to facilitate volitional movement (Cullen 2012). In particular, neuronal sensitivities to dynamic vestibular and proprioceptive stimulation are attenuated, consistent with behaviorally-dependent suppression of these reflex pathways when the animal's goal is to generate voluntary self-motion.

In addition, these VN neurons also likely send ascending projections to the vestibular cerebellum (Cheron et al. 1996; Reisine and Raphan 1992) and thalamus (reviewed in Cullen 2012). As detailed above, the level of integration in the mouse VN appears to be more extensive in rodents than in primates, a difference consistent with the proposal that the more developed primate association neocortex assumes functions performed by a network of sensory areas in lower species (Rapoport 1990, 1999). Indeed, we speculate that multimodal integration in the mouse VN may play a central role in higher-level functions such as self-motion perception and spatial orientation. For instance, a predominant model of the HD cell system is an attractor network that is updated by allocentric HD information of vestibular origin (McNaughton et al. 1991; Skaggs et al. 1995; reviewed in Clark and Taube 2012). While updating by vestibular information is generally thought to be required to ensure that encoded and actual HDs stay in register, our current results establish neurons at the earliest central stage of sensory processing, which do not solely encode vestibular information during self-motion. First, consider unimodal neurons: while they do encode an allocentric vestibular signal during passive motion, their responses during active motion are reduced and reveal the integration of vestibular and egocentric motor information. Next, consider bimodal VN neurons: these neurons integrate allocentric vestibular and egocentric proprioceptive signals even during passive motion and encode additional egocentric motor information during active motion.

There is, in fact, accumulating evidence that motor and proprioceptive influences make important contributions to HD cell responses (Taube and Basset 2003; Wiener et al. 2002). Most notably, the direction signal encoded by HD cells has been shown to anticipate head motion, a feature that would be driven by egocentric motor-related inputs rather than allocentric vestibular (or visual) inputs. The motor-related responses reported in our studies of VN neurons could potentially provide a directional heading signal with anticipatory features. Interestingly, it has been recently shown that motor-based anticipation contributes to optimizing gaze stabilization in rodents during active head motion (King and Shanidze 2011; Shanidze et al. 2012), suggesting motor-based anticipation is a common feature of early vestibular processing in rodent. Furthermore, while HD cell network has been chiefly studied in rat, mouse HD cells may be particularly influenced by egocentric cues (i.e., Yoder and Taube 2009). Accordingly, we speculate that egocentric signals (i.e., proprioceptive and motor-related information) make particularly significant contributions to the representation of direction in HD cells of mice. Future work will be required to understand how these signals are integrated to ensure the robust and functionally appropriate representation of direction in HD cells.

ACKNOWLEDGMENTS

The authors thank Jerome Carriot for key contributions to illustration design, and Jerome Carriot, Mohsen Jamali, Diana Mitchell, Alexis Dale, and Yi Shan Wong for comments on the manuscript. We also thank Mathieu Beraneck for advice in the initial stages of these experiments.

GRANTS

This research was supported by the Hilton J. Mckeown and Clarke McLeod Scholarships in the Faculty of Medicine, McGill University (I. Medrea), Canadian Institutes of Health Research (K. E. Cullen), as well as National Institute of Deafness and Other Communications Disorders Grant DC-002390 (K. E. Cullen).

DISCLOSURES

No conflicts of interest, financial or otherwise, are declared by the author(s).

AUTHOR CONTRIBUTIONS

Author contributions: I.M. performed experiments; I.M. and K.E.C. analyzed data; I.M. and K.E.C. prepared figures; I.M. and K.E.C. drafted manuscript; K.E.C. conception and design of research; K.E.C. interpreted results of experiments; K.E.C. edited and revised manuscript; K.E.C. approved final version of manuscript.

REFERENCES

Akaike T. Neuronal organization of the vestibulospinal system in the cat. *Brain Res* 259: 217–227, 1983.

Anastasopoulos D, Mergner T. Canal-neck interaction in vestibular nuclear neurons of the cat. *Exp Brain Res* 46: 269–280, 1992.

Bagnall MW, McElvain LE, Faulstich M, du Lac S. Frequency-independent synaptic transmission supports a linear vestibular behavior. *Neuron* 23: 343–352, 2008.

Bagnall MW, Stevens RJ, du Lac S. Transgenic mouse lines subdivide medial vestibular nucleus neurons into discrete, neurochemically distinct populations. *J Neurosci* 27: 2318–2330, 2007.

Baker JF. Dynamics and directionality of the vestibulo-collic reflex (VCR) in mice. *Exp Brain Res* 167: 108–113, 2005.

Barresi M, Grasso C, Li Volsi G, Manzoni D. Effects of body to head rotation on the labyrinthine responses of rat vestibular neurons. *Neuroscience* 244: 134–146, 2013.

Beraneck M, Cullen KE. Activity of vestibular nuclei neurons during vestibular and optokinetic stimulation in the alert mouse. *J Neurophysiol* 98: 1549–1565, 2007.

Beraneck M, McKee JL, Aleisa M, Cullen KE. Asymmetric recovery in cerebellar-deficient mice following unilateral labyrinthectomy. *J Neurophysiol* 100: 945–958, 2008.

Borst A, Haag J. Effects of mean firing on neural information rate. *J Comput Neurosci* 10: 213–221, 2001.

Boyle R. Activity of medial vestibulospinal tract cells during rotation and ocular movement in the alert squirrel monkey. *J Neurophysiol* 70: 2176–2180, 1993.

Boyle R, Belton T, McCrea RA. Responses of identified vestibulospinal neurons to voluntary eye and head movements in the squirrel monkey. *Ann N Y Acad Sci* 781: 244–263, 1996.

Boyle R, Pompeiano O. Responses of vestibulospinal neurons to neck and macular vestibular inputs in the presence or absence of the paleocerebellum. *Ann N Y Acad Sci* 374: 373–394, 1981.

Brooks JX, Cullen KE. Multimodal integration in rostral fastigial nucleus provides an estimate of body movement. *J Neurosci* 29: 10499–11051, 2009.

Calabrese DR, Hullar TE. Planar relationships of the semicircular canals in two strains of mice. *J Assoc Res Otolaryngol* 7: 151–159, 2006.

Camp AJ, Callister RJ, Brichta AM. Inhibitory synaptic transmission differs in mouse type A and B medial vestibular nucleus neurons in vitro. *J Neurophysiol* 95: 3208–3218, 2006.

Cherif S, Cullen KE, Galiana HL. An improved method for the estimation of firing rate dynamics using an optimal digital filter. *J Neurosci Methods* 173: 165–181, 2008.

Cheron G, Escudero M, Godaux E. Discharge properties of brain stem neurons projecting to the flocculus in the alert cat. I. Medical vestibular nucleus. *J Neurophysiol* 76: 1759–1774, 1996.

Clark BJ, Taube JS. Vestibular and attractor network basis of the head direction cell signal in subcortical circuits. *Front Neural Circuits* 6: 7, 2012.

Cullen KE. The vestibular system: multimodal integration and encoding of self-motion for motor control. *Trends Neurosci* 35: 185–196, 2012.

Cullen KE, Chen-Huang C, McCrea RA. Firing behavior of brain stem neurons during voluntary cancellation of the horizontal vestibuloocular reflex. II. Eye movement related neurons. *J Neurophysiol* 70: 844–856, 1993.

Cullen KE, McCrea RA. Firing behavior of brain stem neurons during voluntary cancellation of the horizontal vestibuloocular reflex. I. Secondary vestibular neurons. *J Neurophysiol* 70: 828–843, 1993.

Cullen KE, Rey CG, Guitton D, Galiana HL. The use of system identification techniques in the analysis of oculomotor burst neuron spike train dynamics. *J Comput Neurosci* 3: 347–368, 1996.

Escudero M, de la Cruz RR, Delgado-García JMA. physiological study of vestibular and prepositus hypoglossi neurones projecting to the abducens nucleus in the alert cat. *J Physiol* 458: 539–560, 1992.

Faulstich M, van Alphen AM, Luo C, du Lac S, De Zeeuw CI. Oculomotor plasticity during vestibular compensation does not depend on cerebellar LTD. *J Neurophysiol* 96: 1187–1195, 2006.

Freedman EG, Sparks DL. Coordination of the eyes and head: movement kinematics. *Exp Brain Res* 131: 22–32, 2000.

Freedman EG, Sparks DL. Eye-head coordination during head-unrestrained gaze shifts in rhesus monkeys. *J Neurophysiol* 77: 2328–2348, 1997.

Fuchs F, Robinson DA. A method for measuring horizontal and vertical eye movement chronically in the monkey. *J Appl Physiol* 21: 1068–1070, 1966.

Furuya N, Kawano K, Shimazu H. Functional organization of vestibulofastigial projection in the horizontal semicircular canal system in the cat. *Exp Brain Res* 24: 75–87, 1975.

Gdowski GT, Belton T, McCrea RA. The neurophysiological substrate for the cervico-ocular reflex in the squirrel monkey. *Exp Brain Res* 140: 253–264, 2001.

Gdowski GT, McCrea RA. Neck proprioceptive inputs to primate vestibular nucleus neurons. *Exp Brain Res* 135: 511–526, 2000.

Goossens HH, Van Opstal AJ. Human eye-head coordination in two dimensions under different sensorimotor conditions. *Exp Brain Res* 114: 542–560, 1997.

Hayes AV, Richmond BJ, Optican LM. A UNIX-based multiple process system for real-time data acquisition and control. *WESCON Conf Proc* 2: 1–10, 1982.

Jamali M, Milligan J, Joundi R, Cullen KE. *A Comparison of Vestibular Information Processing: Mouse vs. Monkey***.** Program No. 583.20. 2010 Neuroscience Meeting Planner. San Diego, CA: Society for Neuroscience, 2010.

Kasper J, Schor RH, Wilson VJ. Response of vestibular neurons to head rotations in vertical planes. II. Response to neck stimulation and vestibular-neck interaction. *J Neurophysiol* 60: 1765–1778, 1988.

Katoh A, Chapman PJ, Raymond JL. Disruption of learned timing in P/Q calcium channel mutants. *PLos One* 3: e3635, 2008.

King WM, Shanidze N. Anticipatory eye movements stabilize gaze during self-generated head movements. *Ann N Y Acad Sci* 1233: 219–225, 2011.

Kleine JF, Guan Y, Kipiani E, Glonti L, Hoshi M, Büttner U. Trunk position influences vestibular responses of fastigial nucleus neurons in the alert monkey. *J Neurophysiol* 91: 2090–2100, 2004.

Lasker DM, Han GC, Park HJ, Minor LB. Rotational responses of vestibular-nerve afferents innervating the semicircular canals in the C.57BL/6 mouse. *J Assoc Res Otolaryngol* 9: 334–348, 2008.

Malinvaud D, Vassias I, Reichenberger I, Rössert C, Straka H. Functional organization of vestibular commissural connections in frog. *J Neurosci* 30: 3310–3325, 2010.

McCrea RA, Gdowski GT, Boyle R, Belton T. Firing behavior of vestibular neurons during active and passive head movements: vestibulo-spinal and other non-eye-movement related neurons. *J Neurophysiol* 82: 416–428, 1999.

McNaughton BL, Chen L, Markus E. "Dead reckoning," landmark learning, and the sense of direction: a neurophysiological and computational hypothesis. *J Cogn Neurosci* 3: 190–202, 1991.

Nelson AB, Krispel CM, Sekirnjak C, du Lac S. Long-lasting increases in intrinsic excitability triggered by inhibition. *Neuron* 40: 609–620, 2003.

Niven JE, Anderson JC, Laughlin SB. Fly photoreceptors demonstrate energy-information trade-offs in neural coding. *PLoS Biol* 5: e116, 2007.

Noda H, Sugita S, Ikeda Y. Afferent and efferent connections of the oculomotor region of the fastigial nucleus in the macaque monkey. *J Comp Neurol* 302: 330–348, 1990.

Pfanzelt S, Rossert C, Rohregger M, Glasauer S, Moore LE, Straka H. Differential dynamic processing of afferent signals in frog tonic, and phasic second-order vestibular neurons. *J Neurosci* 28: 10349–10362, 2008.

Rapoport SI. How did the human brain evolve? A proposal based on new evidence from in vivo brain imaging during attention and ideation. *Brain Res Bull* 50: 149–165, 1990.

Rapoport SI. Integrated phylogeny of the primate brain, with special reference to humans and their diseases. *Brain Res Brain Res Rev* 15: 267–294, 1999.

Reisine H, Raphan T. Neural basis for eye velocity generation in the vestibular nuclei of alert monkeys during off-vertical axis rotation. *Exp Brain Res* 92: 209–226, 1992.

Robinson FR, Phillips JO, Fuchs AF. Coordination of gaze shifts in primates: brainstem inputs to neck and extraocular motoneuron pools. *J Comp Neurol* 346: 43–62, 1994.

Roy JE, Cullen KE. Brain stem pursuit pathways: dissociating visual, vestibular, and proprioceptive inputs during combined eye-head gaze tracking. *J Neurophysiol* 90: 271–290, 2003.

Roy JE, Cullen KE. Dissociating self-generated from passively applied head motion: neural mechanisms in the vestibular nuclei. *J Neurosci* 24: 2102–2111, 2004.

Roy JE, Cullen KE. Selective processing of vestibular reafference during self-generated head motion. *J Neurosci* 21: 2131–2142, 2001.

Roy JE, Cullen KE. Vestibuloocular reflex signal modulation during voluntary and passive head movements. *J Neurophysiol* 87: 2337–2357, 2002.

Sadeghi SG, Mitchell DE, Cullen KE. Different neural strategies for multimodal integration: comparison of two macaque monkey species. *Exp Brain Res* 195: 45–57, 2009.

Sato H, Ohkawa T, Uchino Y, Wilson VJ. Excitatory connections between neurons of the central cervical nucleus and vestibular neurons in the cat. *Exp Brain Res* 115: 381–386, 1997.

Schonewille M, Gao Z, Boele HJ, Veloz MF, Amerika WE, Simek AA, De Jeu MT, Steinberg JP, Takamiya K, Hoebeek FE, Linden DJ, Huganir RL, De Zeeuw CI. Reevaluating the role of LTD in cerebellar motor learning. *Neuron* 70: 43–50, 2001.

Scudder CA, Fuchs AF. Physiological and behavioral identification of vestibular nucleus neurons mediating the horizontal vestibuloocular reflex in trained rhesus monkeys. *J Neurophysiol* 68: 244–264, 1992.

Sekirnjak C, du Lac S. Intrinsic firing dynamics of vestibular nucleus neurons. *J Neurosci* 22: 2083–2095, 2002.

Sekirnjak C, du Lac S. Physiological and anatomical properties of mouse medial vestibular nucleus neurons projecting to the oculomotor nucleus. *J Neurophysiol* 95: 3012–3023, 2006.

Shaikh AG, Meng H, Angelaki DE. Multiple reference frames for motion in the primate cerebellum. *J Neurosci* 24: 4491–4497, 2004.

Shanidze N, Lim K, Dye J, King WM. Galvanic stimulation of the vestibular periphery in guinea pigs during passive whole body rotation and self-generated head movement. *J Neurophysiol* 107: 2260–2270, 2012.

Skaggs WE, Knierim JJ, Kudrimoti HS, McNaughton BL. A model of the neural basis of the rat's sense of direction In: *Advances in Neural Information Processing Systems*, edited by G Tesauro, DS Touretzky, and TK Leen. Cambridge, MA: MIT, 1995, vol. 7, p. 173–180.

Stahl JS. Using eye movements to assess brain function in mice. *Vision Res* 44: 3401–3410, 2004.

Stahl JS, James RA, Oommen BS, Hoebeek FE, De Zeeuw CI. Eye movements of the murine P/Q calcium channel mutant tottering, and the impact of aging. *J Neurophysiol*: 1588–1607, 2006.

Stahl JS, Simpson JI. Dynamics of abducens nucleus neurons in the awake rabbit. *J Neurophysiol* 73: 1383–1395, 1995.

Stahl JS, Thumser ZC. Dynamics of abducens nucleus neurons in the awake mouse. *J Neurophysiol* 108: 2509–2523, 2012.

Stahl JS, van Alphen AM, De Zeeuw CI. A comparison of video and magnetic search coil recordings of mouse eye movements. *J Neurosci Methods* 99: 101–110, 2000.

Takemura K, King WM. Vestibulo-collic reflex (VCR) in mice. *Exp Brain Res* 167: 103–107, 2005.

Taube JS, Basset JP. Persistent neural activity in head direction cells. *Cereb Cortex* 13: 1162–1172, 2003.

Vidal PP, Degallaix L, Josset P, Gasc JP, Cullen KE. Postural and locomotor control in normal and vestibularly deficient mice. *J Physiol* 559: 625–638, 2004.

Vinje WE, Gallant JL. Sparse coding and decorrelation in primary visual cortex during natural vision. *Science* 287: 1273–1276, 2000.

Wiener SI, Berthoz A, Zugaro MB. Multisensory processing in the elaboration of place and head direction responses by limbic system neurons. *Brain Res Cogn Brain Res* 14: 75–90, 2002.

Wilson VJ, Yamagata Y, Yates BJ, Schor RH, Nonaka S. Response of vestibular neurons to head rotations in vertical planes. III. Response of vestibulocollic neurons to vestibular and neck stimulation. *J Neurophysiol* 64: 1695–1703, 1990.

Yang A, Hullar TE. Relationship of semicircular canal size to vestibular-nerve afferent sensitivity in mammals. *J Neurophysiol* 98: 3197–3205, 2007.

Yoder RM, Clark BJ, Taube JS. Origins of landmark encoding for the brain's navigation system. *Trends Neurosci* 34: 561–571, 2011.

Yoder RM, Taube JS. Head direction cell activity in mice: robust directional signal depends on intact otolith organs. *J Neurosci* 29: 1061–1076, 2009.